Journal of Applied Fluid Mechanics, Vol. 9, No. 3, pp. 1175-1187, 2016.
Available online at www.jafmonline.net, ISSN 1735-3572, EISSN 1735-3645.
DOI: 10.18869/acadpub.jafm.68.228.24174

Analysis of Magnetic Field Effects on Distributed Heat Sources in a Nanofluid-Filled Enclosure by Natural Convection

A. Aghaei†, A. A. Abbasian Arani and F. Abedi

Department of Mechanical Engineering, University of Kashan, Kashan, Iran

†*Corresponding Author Email: AlirezaAghaei21@gmail.com*

(Received October 29, 2014; accepted May 27, 2015)

ABSTRACT

This paper studies the effect of magnetic field on the flow field and heat transfer of nanofluid with variable properties in the square enclosure with two arrangements of heat sources. Based upon numerical predictions, the effects of pertinent parameters such as the Rayleigh number (10^3, 10^4 and 10^5), the Hartmann number (0, 25, 50, 75 and 100) and the solid volume fraction (0 to 4%) on the flow and temperature fields and the heat transfer performance of the enclosure are examined. For the numerical solution of conservation equations, finite volume method and SIMPLER algorithm was used. The results show that the heat transfer rate influenced by district heat sources and it increases with distributing heat sources on the side walls and it increases with an increase of the Rayleigh number and volume fraction, but decreases with an increase of Hartmann number.

Keywords: Nanofluid; Natural convection; Magnetic field; Variable properties; Numerical solution.

NOMENCLATURE

B	magnetic field
c_P	Specific heat
d_f	molecule water diameter of
d_p	nanoparticles diameter of
Ha	Hartmann number
k	Thermal conductivity
L	height of the enclosure
p	pressure
Pr	Prandtl number
Ra	Rayleigh number
S	sum of hot walls length
T	temprature
T_H	hot wall temprature
T_c	cold wall temprature
α	thermal diffiusivity
β	thermal expansion coefficient
μ	viscosity
υ	dynamic viscosity
θ	dimensionless temperature
ρ	density
φ	nanoparticles volume fraction
σ	electrical con-ductivity

Subscripts

Avg	average
c	cold
f	fluid
h	hot
nf	nanofluid
p	particle

1. INTRODUCTION

In the recent decades, laminar natural convection of electrically conducting fluids in the presence of magnetic field has been one of the major interesting research subjects due to its widely engineering, Vives and Perry (1987), Utech and Flemmings (1966). For example it used in solidification processes to weaken the buoyancy driven flows. The phenomena have also been successfully used to control of growing crystals because a magnetic field can help to suppress convective flows. Magneto-hydrodynamics (MHD) is the multi-disciplinary study of the flow of electrically conducting fluids in the presence of electromagnetic fields. Therefore, consideration of MHD has also a greater importance in the study of convection flow, Sivasankaran *et al.* (2011). Okada and Ozoe (1992) measured the heat transfer rates of natural

convection of molten gallium with Prandtl number (Pr) of 0.024 in a cubical enclosure heated from one side wall and cooled from the opposite wall with all other walls are insulated in the presence of different magnetic field direction, and found that the external magnetic field in the vertical direction was more effective than the magnetic field applied parallel to the heated vertical wall. Chamkha (2002) investigated an unsteady, laminar, combined forced-free convection flow in a square cavity in the presence of internal heat generation or absorption and a magnetic field. It has been shown that the flow behavior and the heat transfer characteristics inside the cavity are strongly affected by the presence of magnetic field. Yu *et al*. (2013) investigated numerically the natural convection flows of an electrically conducting fluid under a inclined uniform magnetic field in rectangular cavities, they showed that the heat transfer is not only determined by the strength of the magnetic field, but also influenced by the inclination angle. Obayedullah and Chowdhury (2013) studied a steady natural convection flow in a rectangular cavity containing internally heated and electrically conducting fluid with the non-uniformly heated bottom wall, and they found that the temperature, fluid flow and heat transfer strongly depend on internal and external Rayleigh numbers and Hartmann numbers. Some other works, Hossain *et al.* (2005), Ozoe, Maruo (1987), Rudariah *et al.*, (1995), Xu *et al.* (2006), Jalil and Al-Tae'y (2007), Venkatachalappa and Subbaraya (1993), Sathiyamoorthy and Chamkha (2010), Corcione (2003), Roy and Basak (2006), involve studies on natural convection in enclosures under influence of magnetic field. The common finding of all these studies is a force which effects on the fluid within the enclosure, called Lorentz force.

Convective heat transfer can be enhanced passively by changing flow geometry, boundary conditions, or by enhancing thermal conductivity of the fluid. Various techniques have been proposed to enhance the heat transfer performance of fluids. Nanofluids with enhanced thermal characteristics have widely been examined to improve the heat transfer performance of many engineering applications, Choi (1995). Eastman *et al*. (1996) showed that an increase in thermal conductivity of approximately 60% can be obtained for a nanofluid consisting of water and 5% volume CuO nanoparticles. This is attributed to the increase in surface area due to the suspension of nanoparticles. Keblinski *et al*. (2002) reported on the possible mechanisms of enhancing thermal conductivity, and suggested that the size effect, the clustering of nanoparticles and the surface adsorption could be the major reason of enhancement, while the Brownian motion of nanoparticles contributes much less than other factors since this motion of nanoparticles is too slow to transport significant amount of heat through a nanofluid. Oztop and Abu-Nada (2008) studied heat transfer and fluid flow due to buoyancy forces in a partially heated enclosure using nanofluids with various types of nanoparticles and found heat transfer enhancement at a low aspect ratio. Ghasemi *et al*. (2011) examined the natural convection in an enclosure that is filled with a water– Al2O3 nanofluid and is influenced by a magnetic field. Their results show that the heat transfer rate increases with Rayleigh number, but that decreases with an increase of the Hartmann number. Basak and Chamkha (2012) investigated natural convection for nanofluids confined within square cavities with various thermal boundary conditions, and they observed enhancement of heat transfer with respect to base fluid for all ranges of Rayleigh number for nanofluids. Several other investigations, Kadri *et al.* (2012), Kefayati (2013), Sheikholeslami *et al.* (2012), Ashorynejad *et al.* (2013) and Nemati *et al.* (2013) involve studies on natural convection in filled enclosures with nanofluids in the presence of magnetic field. A comprehensive nanofluid simulation study should take account of the structure, shape, size, aggregation and anisotropy of the nanoparticles as well as the type, fabrication process, particle aggregation and deterioration of nanofluids, Ghasemi (2011).

Another way to enhancement the heat transfer and achievement to uniform distribution of temperature in the enclosure, is dividing and distributing heat source which is applied at only on one of the walls, along the other walls of the enclosure. These distributed heat sources induce buoyancy flow locally which results in enhanced overall thermal mixing in the enclosure. There are a considerable number of studies reported on natural convection due to distributed heat sources, and majority of the works are mainly focused on electronic cooling applications, Kaluri and Basak (2010).

Recently, Malvandi *et al.* (2014) and Malvandi *et al.* (2014) performed an analytical investigation of nanofluid flow on stretching sheet. Ganji and Malvandi (2014) examined nanofluid natural convection in vertical enclosure influenced by magnetic field. Kaluri *et al.* (2010) studied an alternative energy-efficient method of distributed heating of the cavity by natural convection for various fluids and they found that thermal management policy of distributed heating significantly influences the thermal mixing and temperature uniformity in the enclosures. Kaluri *et al*. (2010) studied efficient thermal mixing of laminar natural convective flow in a square cavity with distributed heat sources and they found that the distributed heat sources play major role for processing of molten materials and gaseous substances.

In the recent studies, for numerical simulation of nanofluids, some beneficial and useful methods, such as CFVEM and LBM with single-phase model were used. Sheikholeslami and Ganji, have many studies about this field, Sheikholeslami and Ganji (2014), (2015), Sheikholeslami (2014), Sheikholeslami *et al.* (2014), Sheikholeslami *et al.* (2014), Sheikholeslami *et al.* (2014), Sheikholeslami *et al.* (2013). Also recently, in flow field and heat transfer of nanofluids modeling,

nanofluids are also considered as two-phases fluid, Sheikholeslami *et al.* (2014), Sheikholeslami *et al.* (2014), Sheikholeslami and Ganji (2014), Sheikholeslami *et al.* (2013). Using the numerical methods and two-phases modeling, helps to develop nanofluids concepts.

To the best knowledge of authors, no studies that investigated the magnetic field effects on the natural convection in nanofluid-filled enclosure with distributed heat sources have been reported. The object of this study is to investigate the effects of magnetic field applied on a square cavity filled by water-CuO nanofluid with two different thermal boundary conditions (fig. 1, A: case 1 and B: case 2).

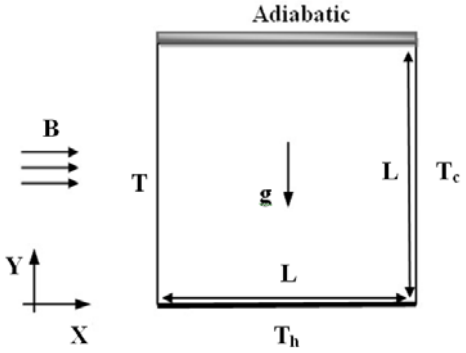

A: Case 1

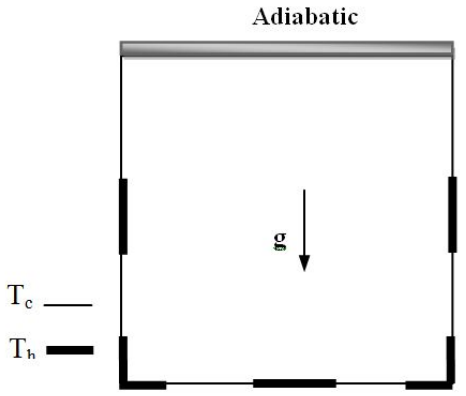

B: Case 2

Fig. 1. schematic diagrams of the physical model and buondary conditions.

2. GOVERNING EQUATIONS AND BOUNDARY CONDITIONS

The physical domain of various cases is shown in fig. 1 (A: case 1, B: case 2). case 1 involved a top adiabatic wall, two cold walls at the left and right sides, and an isothermal heat source which applied uniformly along the bottom wall of enclosure (fig. 1(A: case 1)). In the second case, the isothermal heat source in case 1 divided and applied at the central portion of the bottom and side walls and at the lower corners of enclosure (fig. 1(B: case 2)). In all of the cases the total length of heat sources is equal to 1.

Enclosure is filled by CuO-water nanofluid. In table 1 the values of specific heat, density, thermal conductivity, thermal expansion coefficient and viscosity, given by Hawang *et al*. (2007) and Ogut (2009), are reported for water and CuO. In the current analysis, a two-dimensional laminar model for incompressible and Newtonian fluid is considered. No-slip boundary conditions are assumed at the solid boundaries.

Table 1 Physical properties for pure ware and CuO, Hwang *et al.* (2007) and Ogut (2009)

	β (K^{-1})	k ($Wm^{-1}K^{-1}$)	c_p ($jkg^{-1}K^{-1}$)	ρ (kgm^{-3})
water	$10^4\times2.1$	0.613	4179	997.1
CuO	$10^{-5}\times1.5$	76.5	535.1	6320

Governing equations of continuity (1), momentum (2,3) and energy (4) for a laminar steady-state two-dimensional natural convection flow are:

$$\frac{\partial u}{\partial x}+\frac{\partial v}{\partial y}=0 \tag{1}$$

$$u\frac{\partial u}{\partial x}+v\frac{\partial u}{\partial y}=-\frac{1}{\rho}\frac{\partial p}{\partial x}+\frac{1}{\rho}[\frac{\partial}{\partial x}(\mu\frac{\partial u}{\partial x})+\frac{\partial}{\partial y}(\mu\frac{\partial u}{\partial y})] \tag{2}$$

$$u\frac{\partial v}{\partial x}+v\frac{\partial v}{\partial y}=-\frac{1}{\rho}\frac{\partial p}{\partial y}+\frac{1}{\rho}[\frac{\partial}{\partial x}(\mu\frac{\partial v}{\partial x})+\frac{\partial}{\partial y}(\mu\frac{\partial v}{\partial y})]+\frac{(\rho\beta)}{\rho}g(T-T)-\sigma B v \tag{3}$$

$$u\frac{\partial T}{\partial x}+v\frac{\partial T}{\partial y}=\frac{1}{(\rho c)}[\frac{\partial}{\partial x}(k\frac{\partial T}{\partial x})+\frac{\partial}{\partial y}(k\frac{\partial T}{\partial y})] \tag{4}$$

The stream function presented by:

$$\psi(x,y)=\int u\,dy+\psi_0 \tag{5}$$

By using the following dimensionless variables (6), dimensionless equations for equations (1-5) are:

$$Y=\frac{y}{L},\ S=\frac{s}{L},U=\frac{uL}{\alpha},V=\frac{vL}{\alpha},\ P=\frac{pL}{\rho\alpha}$$
$$\mathrm{Ha}=B\sqrt{\frac{\sigma}{\rho\nu}},\ \theta=\frac{T-T}{T-T},\ \Delta T=T-T \tag{6}$$

Using the mentioned dimensionless variables, governing equations and entropy generation relations can be written in non-dimensional form (7)-(12).

$$\frac{\partial \mathrm{U}}{\partial \mathrm{X}}+\frac{\partial \mathrm{V}}{\partial \mathrm{Y}}=0 \tag{7}$$

$$U\frac{\partial U}{\partial X}+V\frac{\partial U}{\partial Y}=-\frac{\partial P}{\partial X}+\frac{1}{\rho_{nf}\alpha_f}\frac{\partial}{\partial X}\left(\mu_{nf}\frac{\partial U}{\partial X}\right)+\frac{\partial}{\partial Y}\left(\mu_{nf}\frac{\partial U}{\partial Y}\right) \quad (8)$$

$$U\frac{\partial V}{\partial X}+V\frac{\partial V}{\partial Y}=-\frac{\partial P}{\partial Y}+\frac{1}{\rho_{nf}\alpha_f}\left[\frac{\partial}{\partial X}\left(\mu_{nf}\frac{\partial U}{\partial X}\right)+\frac{\partial}{\partial Y}\left(\mu_{nf}\frac{\partial U}{\partial Y}\right)\right]+\frac{(\rho\beta)_{nf}}{\rho_{nf}\beta_f}Ra\,\mathrm{Pr}\,\theta-\mathrm{Ha}^2\times\mathrm{pr}\times V \quad (9)$$

$$U\frac{\partial \theta}{\partial X}+V\frac{\partial \theta}{\partial Y}=\frac{1}{(\rho c_p)_{nf}\alpha_f}\left[\frac{\partial}{\partial X}\left(k_{nf}\frac{\partial \theta}{\partial X}\right)+\frac{\partial}{\partial Y}\left(k_{nf}\frac{\partial \theta}{\partial Y}\right)\right] \quad (10)$$

f and nf subscripts are corresponding base fluid and nanofluid, respectively.

And the dimensionless stream function is:

Dimensionless stream function is defined as (11).

$$\Psi(X,Y)=\int UdY \quad (11)$$

In respect to geometry, boundary conditions are:

$$\begin{aligned}&U(X,0)=U(X,1)=U(0,Y)=U(1,Y)=0\\&V(X,0)=V(X,1)=V(0,Y)=V(1,Y)=0\\&\theta=1\text{ (for hot region)}\\&\theta=0\text{ (for cold region)}\\&\frac{\partial\theta}{\partial Y}=0\text{ (for adiabatic top wall)}\end{aligned} \quad (12)$$

Nanofluid characteristics as density, heat capacitance, thermal expansion coefficient, thermal diffusivity, static part of viscosity, Brinkman (1952), and thermal conductivity, Maxwell (1873) and effective dynamic viscosity can be attained by (13-20) equations:

$$\rho_{nf}=(1-\varphi)\rho_f+\varphi\rho_s \quad (13)$$

$$(\rho c_p)_{nf}=(1-\varphi)(\rho c_p)_f+\varphi(\rho c_p)_s \quad (14)$$

$$(\rho\beta)_{nf}=(1-\varphi)(\rho\beta)_f+\varphi(\rho\beta)_s \quad (15)$$

$$\alpha_{nf}=\frac{k_{nf}}{(\rho c_P)_{nf}} \quad (16)$$

$$\mu_{Static}=\mu_f(1-\varphi)^{-2.5} \quad (17)$$

$$k_{Static}=k_f\left[\frac{(k_s+2k_f)-2\varphi(k_f-k_s)}{(k_s+2k_f)+\varphi(k_f-k_s)}\right] \quad (18)$$

$$\mu_{eff}=\mu_{Static}+\mu_{Brownian} \quad (19)$$

$$k_{eff}=k_{Static}+k_{Brownian} \quad (20)$$

Where $\mu_{Brownian}$ and $k_{Brownian}$ defined as Koo and. Kleinstreuer (2004), Koo and Kleinstreuer (2005).

$$\mu_{Brownian}=5\times10^4\lambda\varphi\rho_f\sqrt{\frac{\kappa T}{2\rho_s R_s}}\xi(T,\varphi) \quad (21)$$

$$k_{Brownian}=5\times10^4\lambda\varphi\rho_f c_{p,f}\sqrt{\frac{\kappa T}{2\rho_s R_s}}\xi(T,\varphi) \quad (22)$$

ρ_s and R_s (23.5×10^{-9} m) are density and radius of nanoparticles respectively and κ is Boltzmann constant $\left(\kappa=1.3807\times10^{-23}\,J/K\right)$. For λ and ζ functions which experimentally estimated for $300<T(K)<325$, for water-CuO nanofluid are:

$R_s$and $\rho_s$are radius and density of nanoparticles, respectively, and κ is Boltzmann constant (κ=1.3807×10-23 J/k). For CuO-water nanofluid, ξ and λ functions which are experimentally estimated at the range of 300< T(k)< 325are (Aminossadati 2011).

$$\begin{aligned}&\lambda=0.0137(100\varphi)^{-0.8229}\ for\ \varphi\le1\%\\&\lambda=0.0011(100\varphi)^{-0.7272}\ for\ \varphi>1\%\end{aligned} \quad (23)$$

$$\xi(T,\varphi)=(-6.04\varphi+0.4705)T+(1722.3\varphi-134.63)\quad for\ \ 1\%\le\varphi\le4\% \quad (24)$$

The effect of Brownian motion with considering the influence of temperature appears in (17) and (18) equations.

electrical conductivity of the nanofluid is defined as:

$$\frac{\sigma_{nf}}{\sigma_f}=1+\frac{3(\frac{\sigma_p}{\sigma_f}-1)\varphi}{(\frac{\sigma_p}{\sigma_f}+2)-(\frac{\sigma_p}{\sigma_f}-1)\varphi} \quad (25)$$

The convective heat transfer coefficient is:

$$h_{nf}=\frac{q}{T_h-T_c} \quad (26)$$

The Nusselt number according to height of enclosure presented by:

$$\mathrm{Nu}=\frac{h_{nf}L}{k_f} \quad (27)$$

L is height of cavity. The heat flux is:

Wall heat flux per unit area is defined as (28).

$$q=-k_{nf}\frac{T_h-T_c}{L}\frac{\partial\theta}{\partial S} \quad (28)$$

With replacing (26) and (28) into (27), the Nusselt number is:

$$\mathrm{Nu}=-\left(\frac{k_{nf}}{k_f}\right)\frac{\partial\theta}{\partial S} \quad (29)$$

And the average Nusselt number at hot wall is:

$$\mathrm{Nu}_{Avg}=\frac{1}{S}\int_{on\ all\ hot\ zone}\mathrm{Nu}\,dS \quad (30)$$

3. NUMERICAL APPROACH AND VALIDATION

Governing equations solved by utilizing finite volume method and SIMPLER algorithm (Fig. 2).

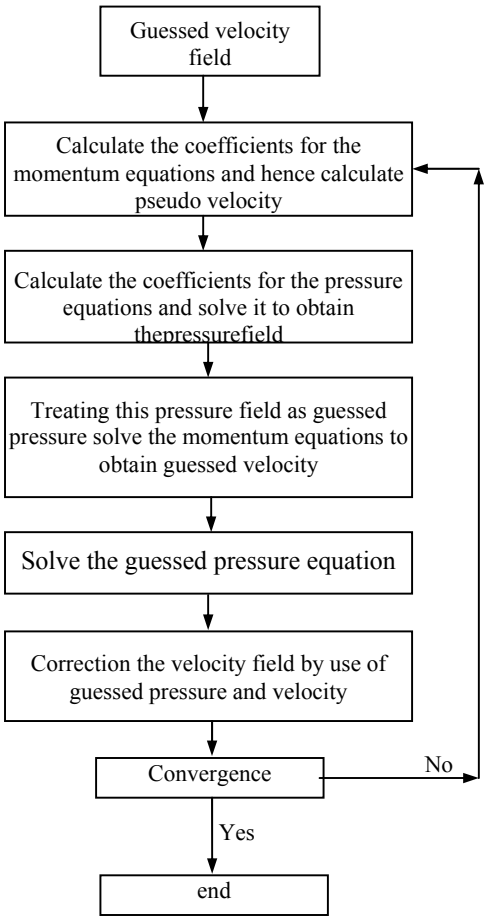

Fig. 2. SIMPLER Algorithm.

Initially, an uniform and appropriate grid considered on the computational domain and then around each node, a control volume is created and by integrating the governing equations over each control volume and differencing equations, a system of algebraic equations is obtained. Second-order central difference scheme is used for the diffusion terms and for convection terms, hybrid method considered. In this method, for Peclet numbers (Pe) smaller than 2, the central difference scheme, and for Pe>2, the upwind finite difference are used. To achieve convergence, under relaxations factors 0.5 for velocity components and 0.7 for temperature are used. For overcome the Checkerboard Pressure field used staggered grid, Patankar (1980).The convergence measure for pressure, velocity and temperature is obtained of equation (31), where M and N are the number of grid points in the x and y direction, respectively and ζ represents the resolved variable k is the number of iterations and the maximum amount of error is 10^{-7}.

$$Error = \frac{\sum_{i=1}^{M}\sum_{j=1}^{N}\left|\zeta_{i,j}^{k+1}-\zeta_{i,j}^{k}\right|}{\sum_{i=1}^{M}\sum_{j=1}^{N}\left|\zeta_{i,j}^{k+1}\right|} \le 10^{-7} \tag{31}$$

3. 1. Grid in Dependenceanalysis

In order to find an appropriate grid which led to the independence of results from the grid, the average Nusselt number for water-CuO nanofluid for grid with various number of nodes for case 1 obtained and compared with together in table 2. Giving the average Nusselt number values, it seems that a 101×101 grid points is suitable.

Table 2 Average Nusselt number on the hot wall for case 1 and water-CuO nanofluid (φ=0.02) at Ra=10^5 and Ha=50 for various numbers of point

points	61×61	81×81	101×101	121×121
Nu_{avg}	8.15	8.56	8.90	9.05

3. 2. Code Validation

In order to validate the results of the computer code, a numerical approach is carried out and its result compared with the results presented in [38, 20] in tables 3 and 4. As can been seen, the relative difference in Nusselt numbers are very small and thus ensure the accuracy of modeling results.

Table 3 Validation of the present study against the results of Aminossadati and Ghsemi (2011) for Nusselt number with different Rayleigh and Hartmann numbers for φ=0.02

Ra	Ha	Present work	Aminossadati, Ghsemi(2011)	Difference percentage
10^3	30	1.182	1.184	0.16
10^4	30	1.290	1.291	0.07
	0	4.966	4.968	0.04
10^5	30	3.107	3.108	0.03
	60	1.805	1.806	0.05

4. RESULTS AND DISCUSSION

Fig. 3, presents streamlines and isotherms for case 1 for both pure water and water-CuO nanofluid (φ=0.02) at different values of Rayleigh and Hartmann number. As streamlines show for all ranges of Rayleigh and Hartmann number that investigated, two symmetric vortexes are created in the enclosure. With increasing Rayleigh number the vortexes become more stretched in the vertical direction and their center is shifted to the middle of enclosure. Vertical vortex stretching indicates an enhancement of convective heat transfer because of increasing Rayleigh number and its effect on buoyant force. With increasing Hartmann number at a fixed Rayleigh number, vortex center is shifted to the lower part of enclosure, and near the hot bottom wall, the dense of streamlines increases. This

behavior of streamlines shows convective heat transfer decreases by increasing of Hartmann number and nature of hear transfer is more close to conductive heat transfer, at lower Rayleigh numbers specially. Magnetic field strength increases with increasing Hartmann number. Lorentz force resulting from the applied magnetic field, which is due to the downward direction of magnetic field acts as a resisting force against the motion of nanofluid which is influenced by buoyancy force and prevents the natural convection.

Table 4 Validation of the present study against the results of Oztop and Abu-Nada (2008) for Nusselt number with different Rayleigh numbers and volume faractions

Ra	φ	Present work	Oztop and Abu-Nada (2008)
10^3	0.00	1.008	1.004
	0.10	1.253	1.251
	0.20	1.600	1.627
10^5	0.00	3.993	3.983
	0.10	4.459	4.440
	0.20	4.861	4.875

Isothermal lines at Rayleigh numbers of 103 and 104 in the bottom corners of enclosure are agglomerated and with increasing the Rayleigh number to 105 the density of lines can be observed throughout whole bottom wall. With increasing Rayleigh number and thus enhancement of natural convection of nanofluid, heat transfer increases and congestion of isotherms confirms this object too. With increasing Rayleigh number, the isotherms which were in the middle of the enclosure at $Ra=10^3$ inclined to side walls and lines agglomerate reduce in the middle of enclosure. At $Ra=10^3$, with increasing Hartmann number no change in the behavior of isotherms is observed. Given that in this Rayleigh number, effect of natural convection is low and flow behavior is more closely to thermal conduction, increasing strength of magnetic field that reduces the natural convection of nanofluid, has no noticeable effect on streamlines. At $Ra=10^4$, 10^5 and Ha=0, isotherms are more curved. Curved lines indicate rising motion and convection of nanofluid. Curvature of isothermal lines reduces with increasing Hartmann number, which presents a decrease of nanofluid convection.

In fig. 4 the streamlines and isotherms for both pure water and nanofluid (φ=0.02) at different values of Rayleigh and Hartmann number for case 2 is shown. Affect the distribution of heat sources, a large number of vortexes can be seen at enclosure walls. In this case same as the first case, with increasing Hartmann number, natural convection decreases and thermal conductivity is dominant behavior. With an increase of the Hartmann number at fixed Rayleigh number, vortexes tend to the lower part of enclosure and the small vortexes forming at the lower corners of enclosure are bigger and stronger. This behavior is seen at all Rayleigh numbers with increasing Hartmann number. Isotherm lines at the vicinity of heat sources have more density which shows enhancement of heat transfer in these areas. In this case, same as the first case, with increasing Hartmann number, the curvature of isothermal lines reduced. As already mentioned, at low Rayleigh numbers such as $Ra=10^3$, an increase of the magnetic force, due to the reducing of nanofluid motion, does not have much impact on the isothermal lines.

In fig. 5, the vertical component of velocity in the horizontal mid-section is shown for various Hartmann numbers at $Ra=10^5$. In the first case, the values of the vertical component of the dimensionless velocity amplitude greater changes than case 2, which indicates that in case 1, natural convection of nanofluid is more than case 2. Couse of these changes depends on the distribution of hear sources in the enclosure. In both case, with increasing Hartmann number, the velocity values reduce and even in the middle of enclosure is almost no movement in nanofluid. In case 2, due to being heat sources on the vertical side walls in addition the bottom wall, the intensity of reduction of velocity values decreases with increasing Hartmann number comparing with case 1. In both case 1 and 2, manner of velocity changes at the side walls maintained with increasing Hartmann number. This means at high Hartmann numbers, peak of the velocity observed at the sides as well as middle area of enclosure. This shows in this geometry and boundary conditions investigated in this study, increasing Hartmann number does not affect how velocity changes and it only effects on values of velocity. It should be noted that increasing of magnetic field strength depend on the geometry, can generally affect how the velocity changes.fig. 6 shows the maximum value of the stream function in terms of volume fraction for different Hartmann and Rayleigh numbers. At Ha=0, in both case 1 and 2, maximum value of stream function as a measure of flow strength at a fixed Rayleigh number, does not change with increasing volume fraction of nanofluid. In fact, at a fixed Rayleigh number, with increasing volume fraction of the nanoparticles, maximum value of stream function slightly reduces because of increased viscosity due to the increasing volume fraction. On the other hand, it is clear that with increasing Rayleigh number which represents the enhancement in convection and strength of flow, the maximum value of stream function should be increased. With increasing Hartmann number at $Ra=10^5$, a greater reduction in the maximum value of stream function with increasing volume fraction of nanoparticles observed compared with other Rayleigh numbers. This behavior is due to the greater influence of magnetic field on the behavior of nanofluid at high Rayleigh numbers. As a general conclusion in this section can be state that in all ranges of Rayleigh numbers and both cases studied, with increasing Hartmann number, the maximum value of stream function reduces

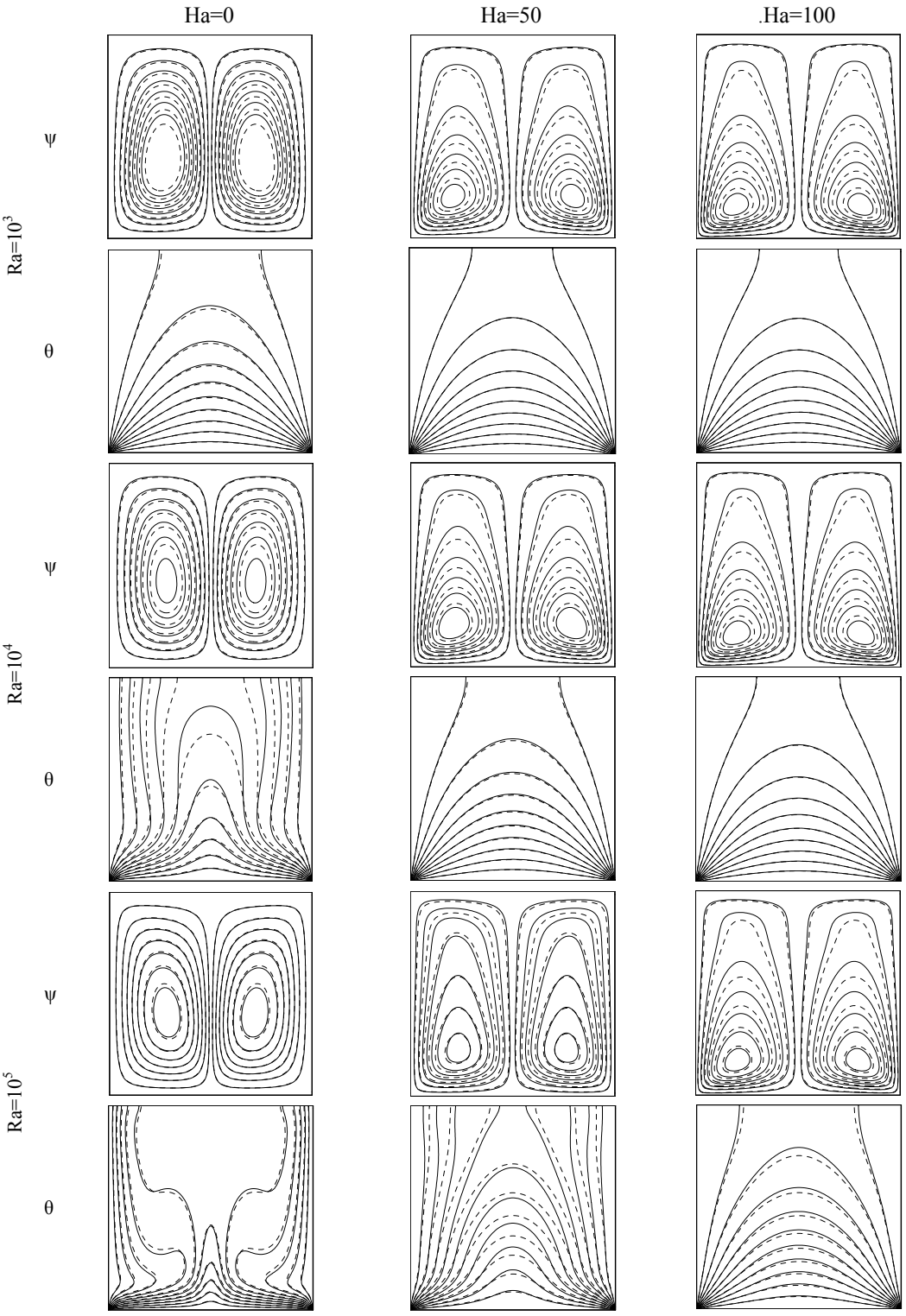

Fig. 3. Streamlines and isotherms for different Ra (—: nanofluid with ϕ =0.02 and - - -: pure water) for case 1.

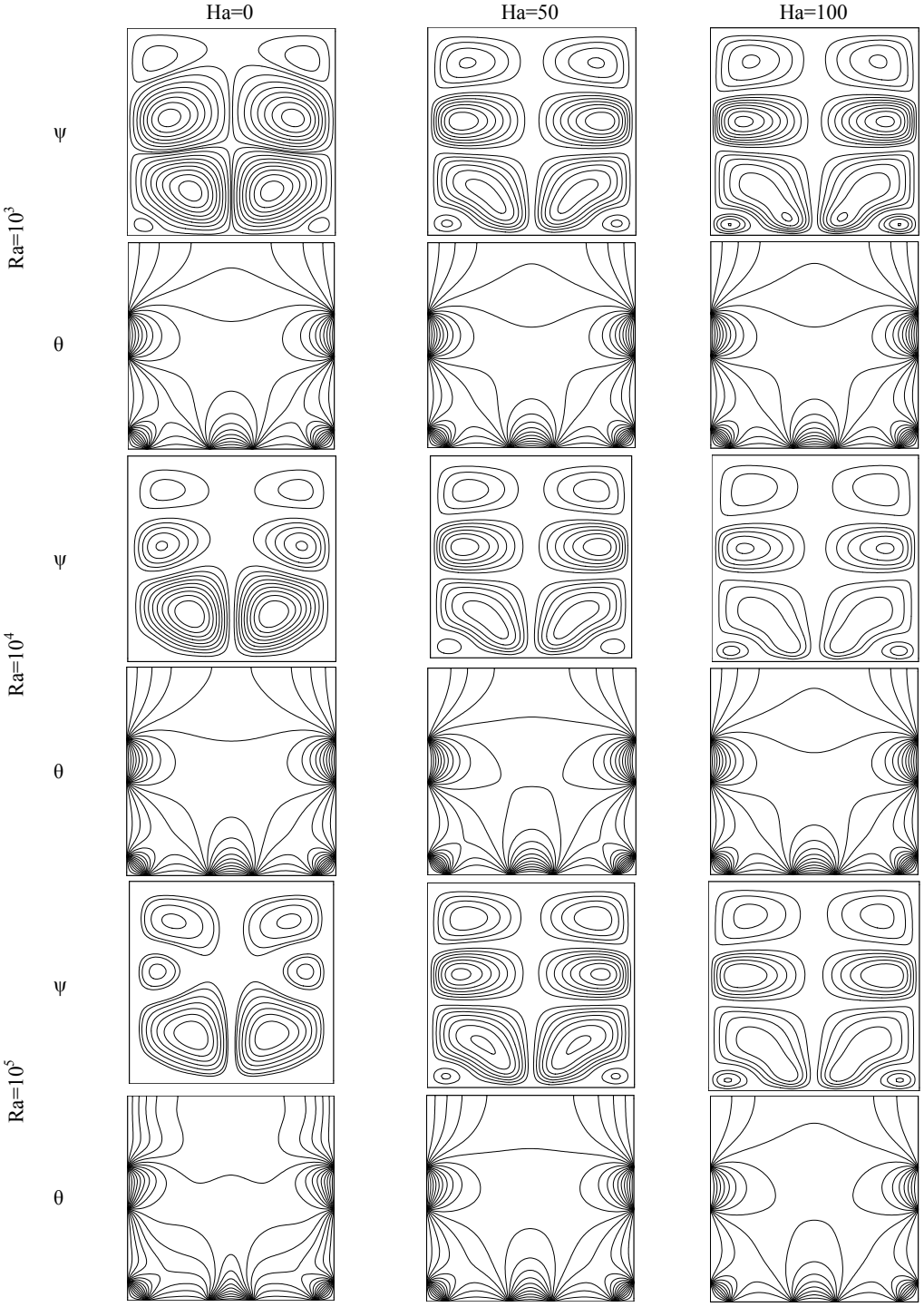

Fig. 4 Streamlines and isotherms for different Ra (—: nanofluid with ϕ=0.02 and - - -: pure water) for case 2.

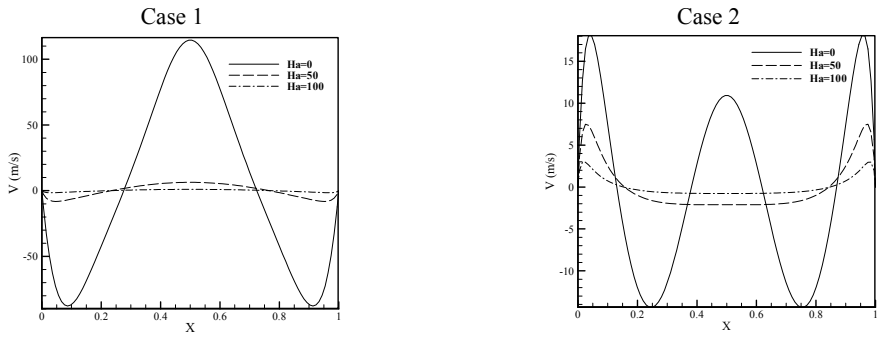

Fig. 5. Variation of vertical component of velocity at the mid-section of the cavity for different Ha and $Ra=10^5$.

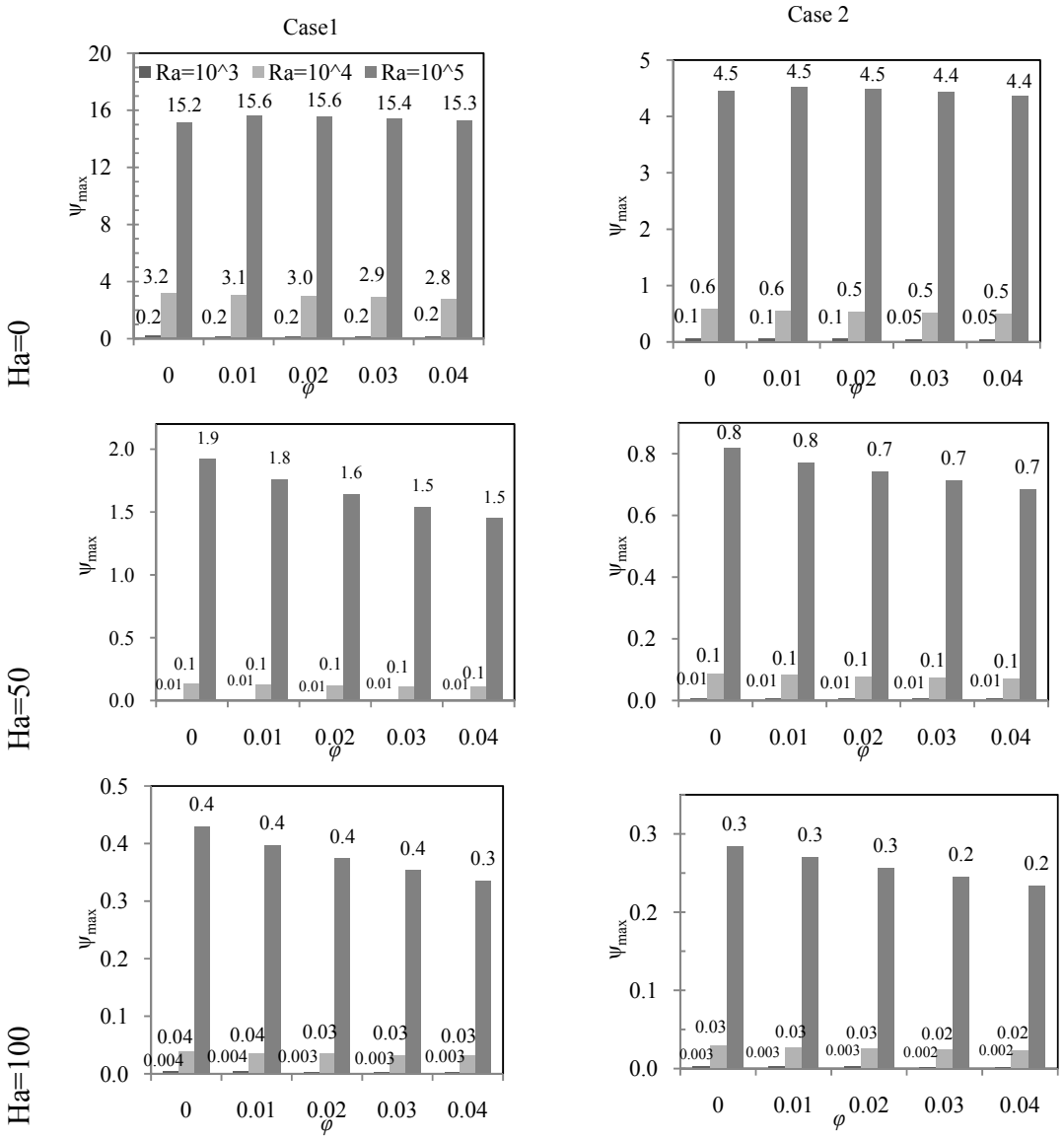

Fig. 6. Maximum value of the stream function in terms of volume fraction for different Hartmann and Rayleigh numbers.

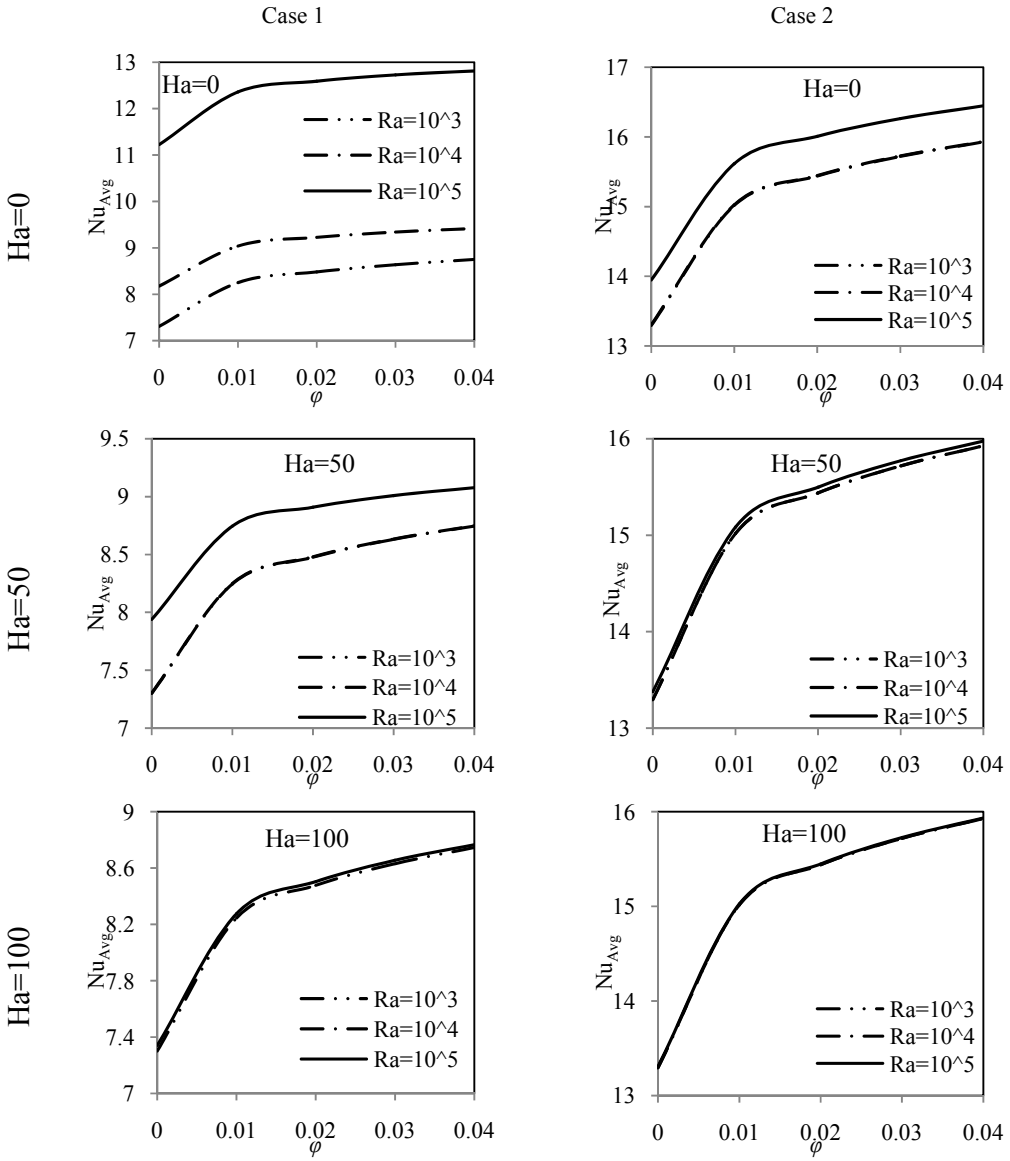

Fig. 7. Variation of Nusselt number in terms of volume fraction for different Hartmann and Rayleigh numbers.

Fig. 7 represents the variation of Nusselt number in terms of volume fraction for different Hartmann and Rayleigh numbers. In all ranges of Hartmann and Rayleigh number investigated and for both cases 1 and 2, the average Nusselt number increases with increasing volume fraction of nanoparticles. Given increasing volume fraction of nanoparticles results increasing of thermal conductivity of nanofluid, thus enhancement in heat transfer, increase of Nusselt number is reasonable. Also for all ranges of Hartmann and Rayleigh number that studied in this article, the average Nusselt numbers for case 2 is greater than average Nusselt numbers for case 1 in similar situations. With increasing Hartmann number, the average Nusselt number values at studied Rayleigh numbers for both case 1 and 2, get closer together. So that the average Nusselt number for Ha=100 for all Rayleigh numbers are almost identical and the curves of variations are coincide. This is another reason that indicates the increased strength of the magnetic field and thereby increase the Lorentz force suppresses natural convection of nanofluid and the nature of heat transfer is near to thermal conduction mostly Consequently, at high Hartmann numbers, the behavior of nanofluid has little dependence on the value of the Rayleigh number. In the second case, the intensity of the magnetic field effect on the average Nusselt number changes depending on the volume fraction is higher, and as it can be seen, the curves of Nusselt number at lower Hartmann number are consistent with

each other.

In fig. 8, the average Nusselt number changes in terms of Hartmann number for both cases 1 and 2 at φ=0.02, to better understand the dependence of the Nusselt number changes on Hartmann number are shown. At Ra=10^3 for both cases 1 and 2, with increasing Hartmann number, the average Nusselt number does not change appreciably. Couse of this behavior is weaker natural convection of nanofluid at Ra=10^3. At Ra=10^4 with increasing Hartmann number to 20, the average Nusselt number drastically reduces but then with increasing Hartmann number, Nusselt

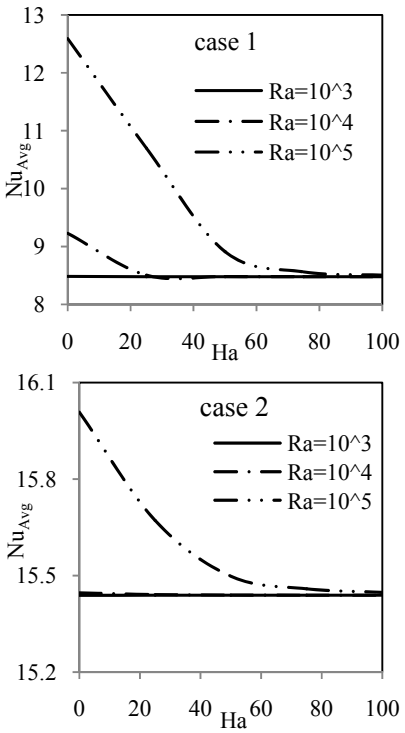

Fig. 8. Average Nusselt number changes in terms of Hartmann number for both cases 1 and 2 at φ=0.02.

number does not change. In fact, although at Ra=10^4, natural convection of nanofluid is stronger than Ra=10^3, but the buoyancy force is still weak, so even at low Hartmann numbers such as 20, natural convection suppressed and heat transfer is approaching to thermal conduction mostly, so increasing of magnetic field strength does not affect the values of Nusselt number. At Ra=10^5 and Ha=60, behavior of nanofluid is close to thermal conductivity and then increasing Hartmann number does not influence the Nusselt number.

5. CONCLUSION

In this study the effect of magnetic field on the flow field and heat transfer of nanofluid with variable properties in the square enclosure with two arrangements of heat sources was investigated. The study was conducted for Rayleigh numbers 10^3, 10^4 and 10^5 and Hartmann numbers 0, 25, 50, 75 and 100 and volume fraction 0 to 4% of nanoparticles. For the numerical solution of conservation equations, finite volume method and SIMPLER algorithm was used. According the studies the following results were obtained:

1) With increasing Hartmann number, the natural convection of nanofluid reduced and behavior of nanofluid approaches to thermal conductivity, at low Rayleigh numbers specially.
2) At low Rayleigh numbers such as 10^3, increasing of magnetic field strength does not have much impact on the flow behavior.
3) In both cases 1 and 2, with increasing Hartmann number, the velocity values reduces and at the middle area of enclosure, the velocity of nanoparticles is almost zero.
4) For all ranges of Rayleigh number and both cases which investigated, with increasing of Hartmann number, maximum value of stream function reduces.
5) At high Hartmann numbers, the behavior of nanofluid does not depend on the Rayleigh number values noticeably.
6) For all ranges of Rayleigh and Hartmann number that investigated, for both cases 1 and 2, the average Nusselt number increases with increasing volume fraction of nanoparticles.
7) With increasing Hartmann number in both cases 1 and 2, the values of average Nusselt number at Rayleigh numbers that studied, get closer together and Nusselt number variation curves are overlapped.
8) When the behavior of nanofluid approaches to thermal conductivity, the increased intensity of the magnetic field does not affect the values of the Nusselt number.

REFERENCES

Aminossadati, S. M. and B. Ghasemi (2011). Natural convection of water–CuO nanofluid in a cavity with two pairs of heat source–sink. *Int. Comm. Heat Mass Transfer* 38, 672–678.

Ashorynejad, H. R. Mohamad, A. A. and M. Sheikholeslami (2013). Magnetic field effects on natural convection flow of a nanofluid in a horizontal cylindrical annulus using Lattice Boltzmann method. *Int. J. Therm*. Sci. 64, 240-250.

Basak, T. and A. J. Chamkha (2012). Heatline analysis on natural convection for nanofluids confined within square cavities with various thermal boundary conditions. *Int. J. Heat Mass Transfer* 55, 5526-5543.

Brinkman, H. C. (1952) The viscosity of concentrated suspensions and solution. *J. Chemical Physics* 20, 571–581.

Chamkha, A. J. (2002). hydromagnetic combined convection flow in a vertical lid-driven cavity with internal heat generation or absorption, *Numer. Heat Transfer* A 41, 529-546.

Choi, S. U. S. (1995). Enhancing thermal conductivity of fluids with nanoparticles. *ASME Fluids Eng*. Div 231, 99-105.

Corcione, M. (2003). Effects of the thermal boundary conditions at the sidewalls upon natural convection in rectangular enclosures heated from below and cooled from above. *Int. J. Therm. Sci* 42, 199-208.

Eastman, J. A., U. S. Choi, S. Li, L. J. Thompson and S. Lee (1996). Enhanced Thermal Conductivity through the Development of Nanofluids. *MRS Proc*. 457.

Ghasemi, B., S. M. Aminossadati and A. Raisi (2011). Magnetic field effect on natural convection in a nanofluid-filled square enclosure. *Int. J. Therm. Sci*. 50, 1748-1756.

Hossain, M. A., M. Z. Hafizb and D. A. S. Ress (2005). Buoyancy and thermocapillary driven convection flow of an electrically conducting fluid in an enclosure with heat generation. *Int. J. Therm. Sci* 44, 676-684.

Hwang, Y., J. K. Lee, C. H. Lee, Y. M. Jung, S. I. Cheong, C. G. Lee, B. C. Ku and S. P. Jang (2007). Stability and thermal conductivity characteristics of nanofluids. *Thermo chimica Acta* 455(1–2), 70–74.

Jalil, J. M. and K. A. Al-Tae'y (2007). The Effect of Nonuniform Magnetic Field on Natural Convection in an Enclosure. *Numer. Heat Transfer A* 51, 899-917.

Kadri, S., R. Mehdaoui and M. Elmir (2012). A Vertical magneto-convection in square cavity containing a Al_2O_3+water nanofluid: cooling of electronic compounds. *Eng. Proc* 18, 724–732.

Kaluri, R. S. and T. Basak (2010). Analysis of distributed thermal management policy for energy-efficient processing of materials by natural convection. *Eng*. 35, 5093-5107.

Kaluri, R. S., T. Basak and S. Roy (2010). Heatline approach for visualization of heat flow and efficient thermal mixing with discrete heat sources. *Int. J. Heat Mass Transfer* 53, 3241–3261.

Keblinski, P., S. R. Phillpot, S. U. S. Choi and J. A. Eastman (2002). Mechanisms of heat flow in suspensions of nano-sized particles (nanofluids). *Int. J. Heat Mass Transfer* 45, 855-863.

Kefayati, GH. R. (2013). Lattice Boltzmann simulation of MHD natural convection in a nanofluid-filled cavity with sinusoidal temperature distribution. *Powder Tech* 243, 171–183.

Koo, J. and C. Kleinstreuer (2005). Laminar nanofluid flow in microheat-sinks. *Int. J. Heat Mass* 48(13), 2652–2661.

Koo, J. and C. A. Kleinstreuer (2004). new thermal conductivity model for nanofluids. *J. Nanoparticle Research* 6(6), 577–588.

Malvandi, A., F. Hedayati and M. R. H. Nobari (2014). An Analytical Study on Boundary Layer Flow and Heat Transfer of Nanofluid Induced by a Non-Linearly Stretching Sheet. *Journal of Applied Fluid Mechanics* 7(2), 375-384.

Malvandi, A., F. Hedayati and M. R. H. Nobari (2014). An HAM Analysis of Stagnation-Point Flow of a Nanofluid over a Porous Stretching Sheet with Heat Generation. *Journal of Applied Fluid Mechanics* 7(1), 135-145.

Maxwell, J. C. (1873). A Treatise on Electricity and Magnetism, Vol II, *Oxford University Press*, Cambridge, UK.

Nemati, H., M. Farhadi, K. Sedighi, H. R. Ashorynejad and E. Fattahi (2012). Magnetic field effects on natural convection flow of nanofluid in a rectangular cavity using the Lattice Boltzmann model. *Sci. Iranica B* 19(2), 303–310.

Obayedullah, M. and M. M. K. Chowdhury (2013). MHD natural convection in a rectangular cavity having internal energy sources with non-uniformly heated bottom wall. *Proc. Eng* 56, 76-81.

Ogut, E. B. (2009). Natural convection of water-based nanofluids in an inclined enclosure with a heat source. *Int. J. Thermal Sciences* 48(11), 2063–2073

Okada, K. and H. Ozoe (1992). Experimental heat transfer rates of natural convection of molten gallium suppressed under an external magnetic field in either the X, Y, or Z direction. J. *Heat Transfer* 114, 107-114.

Ozoe, H. and M. Maruo (1987). Magnetic and gravitational natural convection of melted silicon two-dimensional numerical computations for the rate of heat transfer. *JSME. Int*. J 30, 774-784.

Oztop, H. F. and E. Abu-Nada (2008). Numerical study of natural convection in partially heated rectangular enclosures filled with nanofluids. *Int. J. Heat Fluid Flow* 29, 1326-1336.

Patankar, S. V. (1980). *Numerical Heat Transfer and Fluid Flow*, Hemisphere, McGraw-Hill, Washington DC.

Roy, S. and T. Basak (2006). Finite element analysis of natural convection flows in a square cavity with non-uniformly heated wall(s). *Int. J. Eng. Sci* 43,

668-680.

Rudariah, N., R. M. Barron, M. Venkatachalappa and C. K. Subbaraya (1995). Effect of a magnetic field on free convection in a rectangular enclosure. *Int. J. Eng. Sci* 33, 1075-1084.

Sathiyamoorthy, M. and A. Chamkha (2010). Effect of magnetic field on natural convection flow in a liquid gallium filled square cavity for linearly heated side wall(s). *Int. J. Therm. Sci* 49, 1856-1865.

Sheikholeslami, M. (2014). KKL correlation for simulation of nanofluid flow and heat transfer in a permeable channel. *Physics Letters A* 378(45), 3331-3339.

Sheikholeslami, M., S. Abelman and D. D. Ganji (2014). Numerical simulation of MHD nanofluid flow and heat transfer considering viscous dissipation. *Int. J. Heat Mass Transfer* 79, 212–222.

Sheikholeslami, M. and D. D. Ganji (2014). Heated permeable stretching surface in a porous medium using Nanofluids. *Journal of Applied Fluid Mechanics* 7(3), 535-542.

Sheikholeslami, M. and D. D. Ganji (2015). Nanofluid flow and heat transfer between parallel plates considering Brownian motion using DTM. Comput. *Methods Appl. Mech. Engrg* 283, 651–663.

Sheikholeslami, M. and D. D. Ganji (2014). Three dimensional heat and mass transfer in a rotating system using nanofluid. *Powder Technology* 253, 789–796.

Sheikholeslami, M., M. Gorji-Bandpay and D. D. Ganji (2012). Magnetic field effects on natural convection around a horizontal circular cylinder inside a square enclosure filled with nanofluid. Int. Comm. *Heat Mass Transfer* 39, 978–986.

Sheikholeslami, M., M. Gorji-Bandpy, D. D. Ganji and S. Soleimani (2014). Thermal management for free convection of nanofluid using two phase model. *Journal of Molecular Liquids* 194, 179–187.

Sheikholeslami, M., M. Gorji-Bandpy and D. D. Ganji (2013). Numerical investigation of MHD effects on Al2O3-water nanofluid flow and heat transfer in a semi-annulus enclosure using LBM. *Energy* 60, 501-510.

Sheikholeslami, M., M. Gorji-Bandpy and D. D. Ganji (2014). Lattice Boltzmann method for MHD natural convection heat transfer using nanofluid. *Powder Technology* 254, 82-93.

Sheikholeslami, M., M. Gorji-Bandpy and D. D. Ganji, P. Rana, S. Soleimani (2014). Magnetohydrodynamic free convection of Al2O3-water nanofluid considering Thermophoresis and Brownian motion effects. *Computers and Fluids* 94, 147–160.

Sheikholeslami, M., M. Gorji-Bandpy and D. D. Ganji S. Soleimani (2014). Heat flux boundary condition for nanofluid filled enclosure in presence of magnetic field. *Journal of Molecular Liquids* 193, 174-184.

Sheikholeslami, M., M.Gorji-Bandpy and S. Soleimani (2013). Two phase simulation of nanofluid flow and heat transfer using heatline analysis. International Comm. *Heat Mass Transfer* 47, 73–81

Sivasankaran, S., A. Malleswaran, J. Lee and P. Sundar (2011). Hydro-magnetic combined convection in a lid-driven cavity with sinusoidal boundary conditions on both sidewalls. *Int. J. Heat Mass Transfer* 54, 512-525.

Utech, H. P. and M. C. Flemmings (1966). Elimination of Solute Banding in Indium Antimonide Crystals by Growth in a Magnetic Field. *J. Appl. Phys* 37, 2021–2024.

Venkatachalappa, M. and C. K. Subbaraya (1993). Natural convection in a rectangular enclosure in the presence of a magnetic field with uniform heat flux from the side walls. *Acta Mech* 96, 13-26.

Vives, C. and C. Perry (1987). Effects of magnetically damped convection during the controlled solidification of metals and alloys. *Int. J. Heat Mass Transfer* 30, 479–496.

Xu, B., B. Q. Li and D. E. Stock (2006). An experimental study of thermally induced convection of molten gallium in magnetic fields. *Int. J. Heat Mass Transfer* 49, 2009-2019.

Yu, P. X., J. X. Qiu, Q. Qin and Z. F. Tian (2013). Numerical investigation of natural convection in a rectangular cavity under different directions of uniform magnetic field. *Int. J. Heat Mass Transfer* 67, 1131-1144.